Origin of Magnetism in early-type stars

Thesis project

Juan Pablo Hidalgo

Supervisor : Dr. Dominik Schleicher

Universidad de Concepción.

March 14, 2023

Stellar structure

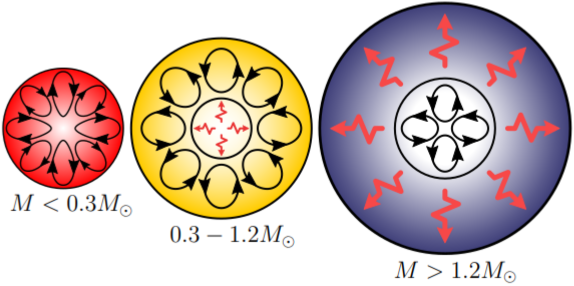

Figure: Diagram of convective and radiative zones for different ranges of stellar masses. Stars with $M \lesssim 0.3M_\odot$ are fully convective, intermediate mass stars have a radiative zone on its core have a radiative zone on its core, and it gets larger as the mass increases. And finally, stars with $M \gtrsim 1.2M_\odot$ are radiative with a convective core (produced by the CNO cycle) (Padmanabhan, 2001).

Astrophysical Dynamos

We refer to a *dynamo* as any process of amplification and maintenance of magnetic fields inside a plasma.

$$\frac{\partial \vec{B}}{\partial t} = \vec{\nabla} \times (\vec{u} \times \vec{B}) + \eta \nabla^2 \vec{B}$$

These processes are most likely to occur inside the convection zones (see Brandenburg & Subramanian 2004), where $u \neq 0$.

Radiative zone?

Ap and Bp stars (1.5 $M_\odot$ to $6M_\odot$) have observable magnetic fields up to 34 kG! (Babcock, 1960).

Possible explanations

The dynamo is driven by the convective core of the star.

Possible explanations

The dynamo is driven by the convective core of the star.

Previous work

A core dynamo was explored by Augustson et al. (2016), who performed 3D simulations of a 10 $M_{\odot}$ B-type star, modeling the inner 64% of its radius. The innermost values of the core were excluded to avoid the coordinate singularity. They found core dynamos able to produce strong magnetic fields, with peaks strengths exceeding a megagauss.

Possible explanations (2)

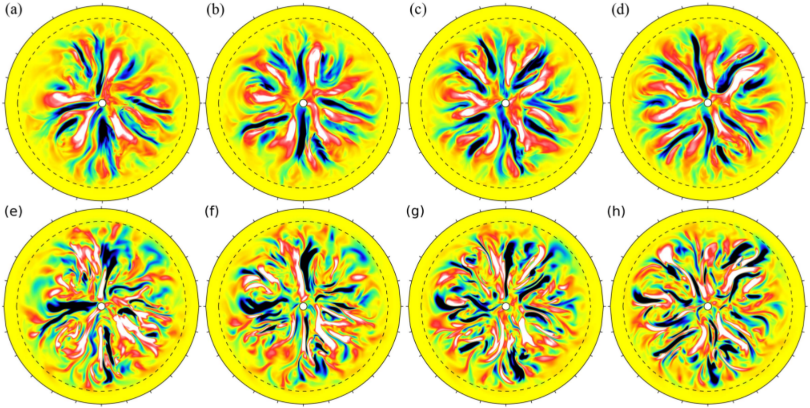

Figure: Time evolution (each plot is 20 days apart) of u_r (top) and B_r (bottom), from the run with $\Omega = 15\Omega_\odot$ in a set of equatorial cuts. Clipping values are ± 100 m s^{-1}, and $\pm 10^5$ G, respectively. Extracted from Augustson et al. (2016).

Possible explanations (3)

Fossil field surviving from the early stages.

Possible explanations (3)

Fossil field surviving from the early stages.

Previous work

Braithwaite & Nordlund (2005) performed 3D simulations of a $2M_\odot$, $R = 1.8R_\odot$ A-type star, inside a box of side $l = 4.5R$ using a grid of 96^3. They found stable magnetic field configurations in a radiative interior starting with random field initial conditions.

Possible explanations (4)

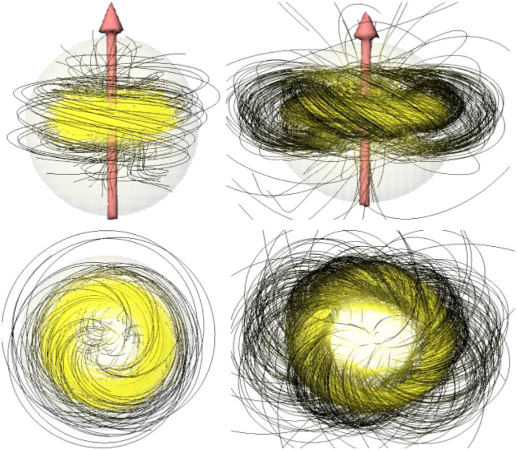

Figure: Snapshots of one of the runs with a stable magnetic field configuration. The upper plots correspond to $t = 22.6$ days (left) and $t = 31.9$ days (right). The lower plots are the same snapshots viewed from a different angle. Extracted from Braithwaite & Nordlund (2005).

Possible explanations (5)

Interaction between a core-dynamo and a fossil field.

Possible explanations (5)

Interaction between a core-dynamo and a fossil field.

Previous work

Featherstone et al. (2009) performed 3D simulations of the inner 30% by radius of a $2M_\odot$ A-type star (excluding the innermost values), modeling a core dynamo surrounded by a radiative envelope. The inclusion of a fossil field in this envelope can lead to a very strong super-equipartition field.

Possible explanations (6)

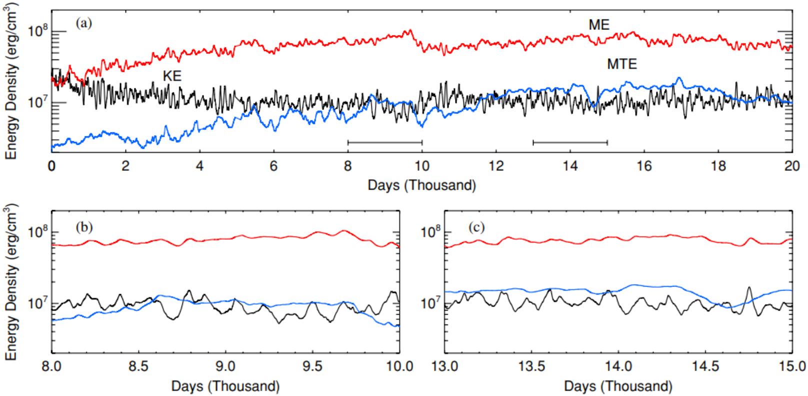

Figure: Temporal evolution of overall energy densities after imposing a mixed poloidal–toroidal magnetic (fossil) field configuration. The magnetic energy (ME) grows until it reaches 10 times the value of the kinetic energy (KE). Extracted from Featherstone et al. (2009).

The project

In this project we will perform 3D MHD simulations of an A-star with a radiative envelope and a convective core.

Objectives:

- Study the fluid motions in its core, and the dynamo it generates.

The project

In this project we will perform 3D MHD simulations of an A-star with a radiative envelope and a convective core.

Objectives:

- Study the fluid motions in its core, and the dynamo it generates.
- Include an initial magnetic field configuration (which resembles a fossil field).

The project

In this project we will perform 3D MHD simulations of an A-star with a radiative envelope and a convective core.

Objectives:

- Study the fluid motions in its core, and the dynamo it generates.
- Include an initial magnetic field configuration (which resembles a fossil field).
- Analyze the interaction between the fossil field and the core-dynamo.

The codes that we will be using, are the following:

The Pencil Code

It is a highly modular high-order finite-difference code for compressible non-ideal Magnetohydrodynamics (Pencil Code Collaboration et al., 2021).

It has been used to explore dynamos coming from different type of stars.

- Navarrete et al. (2019) studied the eclipsing time variations of a binary system modeling a solar mass star.

The Pencil Code

It is a highly modular high-order finite-difference code for compressible non-ideal Magnetohydrodynamics (Pencil Code Collaboration et al., 2021).

It has been used to explore dynamos coming from different type of stars.

- Navarrete et al. (2019) studied the eclipsing time variations of a binary system modeling a solar mass star.
- Käpylä (2021) and Ortiz-Rodríguez et al. (Submitted) performed simulations of a fully convective $0.2 M_{\odot}$ M-dwarf.

The Pencil Code

It is a highly modular high-order finite-difference code for compressible non-ideal Magnetohydrodynamics (Pencil Code Collaboration et al., 2021).

It has been used to explore dynamos coming from different type of stars.

- Navarrete et al. (2019) studied the eclipsing time variations of a binary system modeling a solar mass star.
- Käpylä (2021) and Ortiz-Rodríguez et al. (Submitted) performed simulations of a fully convective $0.2 M_\odot$ M-dwarf.
- Toro et al. (In progress) will model a partially convective low mass star.

MESA

Modules for Experiments in Stellar Astrophysics (Paxton et al., 2010) is an open source one-dimensional stellar evolution code, that allows to model a wide range of stars, ranging from very low mass to massive stars, and even advanced evolutionary phases.

MESA

Modules for Experiments in Stellar Astrophysics (Paxton et al., 2010) is an open source one-dimensional stellar evolution code, that allows to model a wide range of stars, ranging from very low mass to massive stars, and even advanced evolutionary phases.

We will be using the online version MESA-Web, to obtain basic parameters of the star that we will model.

The model (1)

Using THE PENCIL CODE, we will model a massive early-type star of radius R, inside a box of side $l = 2.2R$, where all coordinates (x, y, z) move from $-l/2$ to $l/2$.

The model (1)

Using The Pencil Code, we will model a massive early-type star of radius R, inside a box of side $l = 2.2R$, where all coordinates (x, y, z) move from $-l/2$ to $l/2$.

Choosing different rotation rates Ω_0 based on the Coriolis number (Co ~ 1, Co ~ 2, Co ~ 5), where $\vec{\Omega} = (0, 0, \Omega_0)$.

The model (2)

Solving the non-compressible MHD equations:

$$\frac{\partial \vec{A}}{\partial t} = \vec{u} \times \vec{B} - \eta \mu_0 \vec{J} \tag{1}$$

$$\frac{D \ln \rho}{Dt} = -\vec{\nabla} \cdot \vec{u} \tag{2}$$

$$\frac{D\vec{u}}{Dt} = -\vec{\nabla}\Phi - \frac{1}{\rho}\left(\vec{\nabla} p - \vec{\nabla} \cdot 2\nu\rho \boldsymbol{S} + \vec{J} \times \vec{B}\right) - 2\vec{\Omega} \times \vec{u} + \vec{f}_d \tag{3}$$

$$T\frac{Ds}{Dt} = -\frac{1}{\rho}\left[\vec{\nabla} \cdot (\vec{F}_{\mathrm{rad}} + \vec{F}_{\mathrm{SGS}}) + \mathcal{H} - \mathcal{C}\right] + 2\nu \boldsymbol{S}^2 + \mu_0 \eta J^2 \tag{4}$$

where $D/Dt = \partial/\partial t + \vec{u} \cdot \vec{\nabla}$ is the advective derivative, also $\vec{B} = \vec{\nabla} \times \vec{A}$, the relation between $\vec{J}$ and $\vec{B}$ is given by the Ohm's law $\vec{J} = \vec{\nabla} \times \vec{B}/\mu_0$ and the explicit heating and cooling terms, are extracted from Käpylä (2021).

The model (3)

Radiative energy transfer

Radiation in the stellar interior is approximated as a diffusion process, therefore, the radiative flux is given by:

$$\boxed{\vec{F}_{\text{rad}} = -K\vec{\nabla}T}$$

The size of the radiative zone depends directly on the heat conductivity K, a quantity that is inversely proportional to the opacity κ of the star. Thus, we assumed a constant profile and different initial values for it, which are listed on Table 1.

The model (4)

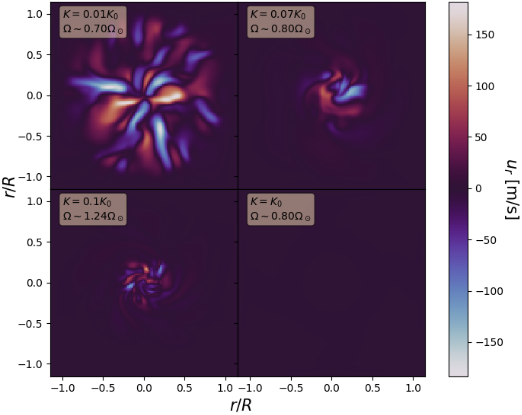

Figure: Snapshots of star-in-a-box simulations, viewing the equatorial plane. The values of the heat conductivity K (where K_0 is the value for a fully radiative configuration) and the rotation rate Ω (in $\Omega_\odot$) are shown in each plot. The colorbar represents the radial component of the flow velocity.

Physical Units

The Pencil Code expresses all the relevant quantities in code units, so to give them physical meaning it is required to do some conversions:

$$[x] = \left(\frac{R_*}{R_{\rm sim}}\right) \qquad [t] = \left(\frac{\Omega_{\rm sim}}{\Omega_*}\right)$$

$$[u] = \left(\frac{\Omega_* R_*}{\Omega_{\rm sim} R_{\rm sim}}\right) \qquad [B] = \left[\frac{\mu_0 \rho_* (\Omega_* R_*)^2}{\mu_{\rm sim} \rho_{\rm sim} (\Omega_{\rm sim} R_{\rm sim})^2}\right]^{1/2}$$

where (see Appendix A of Käpylä et al. 2020):

$$\frac{\Omega_{\rm sim}}{\Omega_*} = L_{\rm ratio}^{1/3} \left(\frac{g_{\rm sim}}{g_*} \frac{R_*}{R_{\rm sim}}\right)^{1/2}$$

Physical Units (2)

The physical parameters of the stars that we will be modeling were extracted from MESA-Web.

Physical Units (2)

The physical parameters of the stars that we will be modeling were extracted from MESA-Web.

For a $2M_\odot$ A-type main sequence star, the 1d-model yields:

$$R_* = 2R_\odot \qquad L_* = 23L_\odot$$

$$\rho_* = 5.6 \cdot 10^4 \text{ kg/m}^3 \qquad g_* = 150 \text{ m/s}^2$$

Diagnostics quantities

Dimensionless parameters:

$$\mathrm{Re} = \frac{u_{\mathrm{rms}}}{\nu k_R} \qquad \mathrm{Re_M} = \frac{u_{\mathrm{rms}}}{\eta k_R}$$

$$\mathrm{Co} = \frac{2\Omega_0}{u_{\mathrm{rms}} k_R} \qquad \mathrm{Pr_M} = \frac{\nu}{\eta}$$

where $k_R = 2\pi/\Delta r$, and Δr is the size of the convective zone.

All simulations have an initial magnetic field seed, given by a Gaussian profile of amplitude $\sim 200\ \mathrm{G}$, and were performed on a grid of 128^3.

Preliminary results (1)

Run	K/K_0	ν [10^9m^2/s]	η [10^9m^2/s]	Ω [$\Omega_\odot$]	$\langle u_{\rm rms}\rangle$ [m/s]	Re	$\mathrm{Re_M}$	$\mathrm{Pr_M}$	$B_{\rm max}$ [kG]
Sim1	0.01	2	1	0.14	126.54	13.51	27.03	2	65.24
$\Delta r \sim 1R$	0.01	2	1	0.70	81.88	8.77	17.54	2	50.46
Sim2	0.04	1.2	1	0.10	117.61	22.17	25.22	1.14	48.84
$\Delta r \sim 1R$	0.04	1.2	1	0.20	95.28	18.03	20.52	1.14	65.36
Sim3 $\Delta r \sim 0.3R$	0.07	0.52	0.31	0.80	265	33.72	56.67	1.68	no dynamo
	0.07	0.2	0.18	0.80	284.35	91.17	101.30	1.11	24.60
	0.07	0.2	0.18	1.58	229.26	73.56	81.73	1.11	26.53
Sim4 $\Delta r \sim 0.2R$	0.1	0.12	0.18	1.24	263.50	96.19	67.33	0.66	24.23
	0.1	0.12	0.18	2.48	177.16	64.67	45.27	0.66	24.04
	0.1	0.12	0.18	6.20	162.27	59.15	41.40	0.66	22.28
	0.1	0.12	0.18	12.40	340.92	124.31	87.01	0.66	no dynamo

Figure: Summary of all the simulations, divided into 4 main groups with different values for the heat conductivity K.

Preliminary results (2)

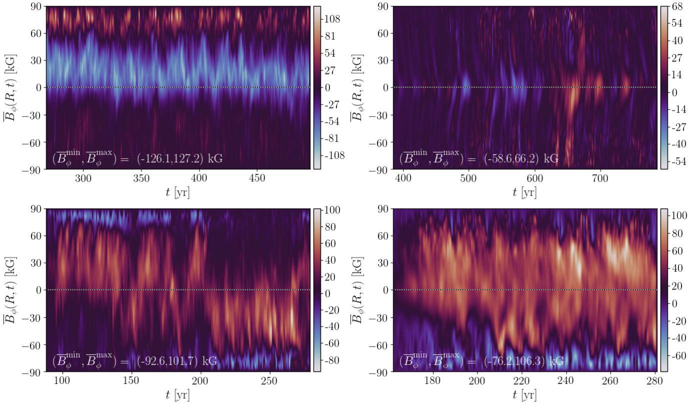

Figure: Azimuthal averaged magnetic field [kG] vs time [year]. The upper panels correspond to Sim1, with $\Omega = 0.14\ \Omega_\odot$ (left) and $\Omega = 0.70\ \Omega_\odot$ (right). The lower panels are the runs from Sim2, $\Omega = 0.10\ \Omega_\odot$ (left) and $\Omega = 0.20\ \Omega_\odot$ (right).

Preliminary results (3)

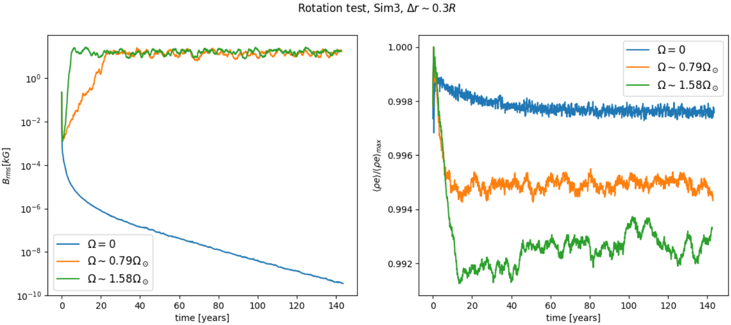

Figure: Root-mean-square magnetic field (left) and normalized mean internal energy (right) vs time, from Sim3 $\Delta r \sim 0.3R$.

Preliminary results (4)

Sim3 $\Delta r \sim 0.3R, \Omega \approx 0.80\Omega_\odot$ (left) and $\Omega \approx 1.58\Omega_\odot$ (right):

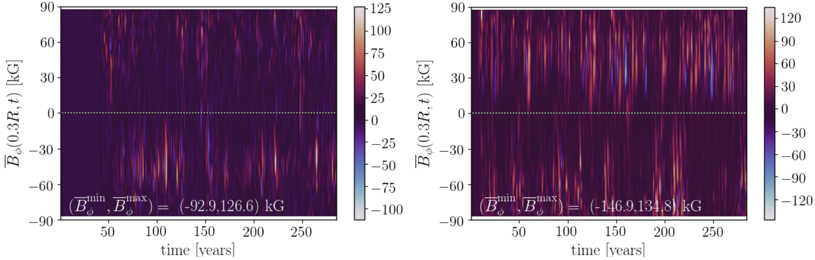

Figure: Azimuthal averaged magnetic field [kG] vs time [yr], at 30% of stellar radius, with $\nu = 2 \cdot 10^8\ \mathrm{m}^2/\mathrm{s}$, $\eta = 1.8 \cdot 10^8\ \mathrm{m}^2/\mathrm{s}$.

Preliminary results (5)

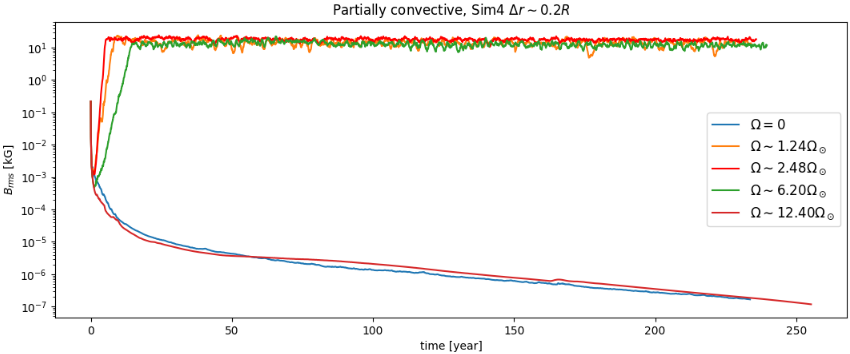

Figure: Root-mean-square magnetic field vs time from Sim4 $\Delta r \sim 0.2R$.

Preliminary results (6)

Sim4 $\Delta r \sim 0.2R$, $\Omega \approx 1.24\Omega_\odot$ (left), and $\Omega \approx 2.48\Omega_\odot$ (right):

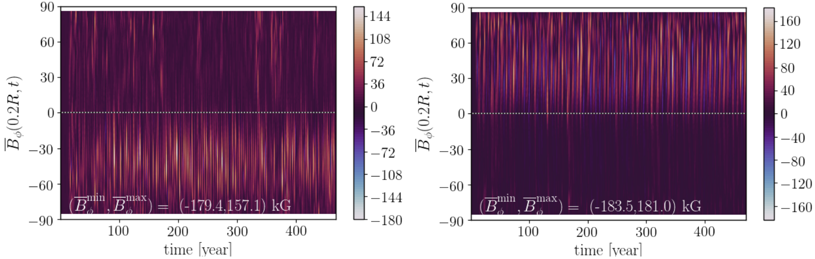

Figure: Azimuthal averaged magnetic field vs time, at 20% of stellar radius.

Preliminary results (7)

Sim4 $\Delta r \sim 0.2R, \Omega \approx 6.20\Omega_\odot$:

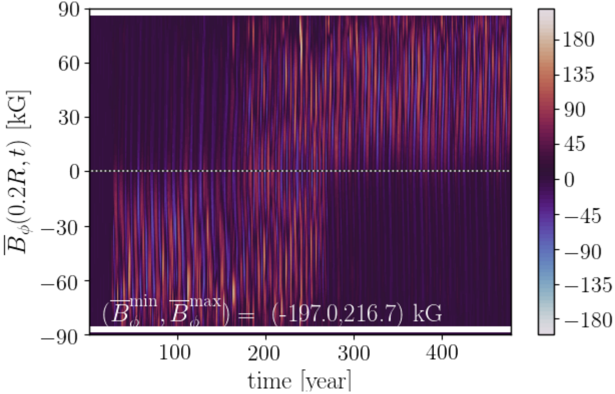

Figure: Azimuthal averaged magnetic field vs time, at 20% of stellar radius.

Preliminary conclusions

Summary

- The model is able to create very strong core dynamos, the most *realistic* simulation set ($\Delta r \sim 0.2R$) have peak values of $(\overline{B}_\phi^{\text{min}}, \overline{B}_\phi^{\text{max}}) = (-197, 216.7)\ \mathrm{kG}$.

Preliminary conclusions

Summary

- The model is able to create very strong core dynamos, the most *realistic* simulation set ($\Delta r \sim 0.2R$) have peak values of $(\overline{B}_{\phi}^{\text{min}}, \overline{B}_{\phi}^{\text{max}}) = (-197, 216.7)\ \mathrm{kG}$.
- The values of B_{rms} are inside the range of the observations: $200\ \mathrm{G} - 30\ \mathrm{kG}$ (Braithwaite & Spruit, 2017).

Preliminary conclusions

Summary

- The model is able to create very strong core dynamos, the most *realistic* simulation set ($\Delta r \sim 0.2R$) have peak values of $(\overline{B}_\phi^{\text{min}}, \overline{B}_\phi^{\text{max}}) = (-197, 216.7)\ \mathrm{kG}$.
- The values of B_{rms} are inside the range of the observations: $200\ \mathrm{G} - 30\ \mathrm{kG}$ (Braithwaite & Spruit, 2017).
- It seems that the core dynamo is not enough to create a large scale magnetic field.

Preliminary conclusions

Summary

- The model is able to create very strong core dynamos, the most *realistic* simulation set ($\Delta r \sim 0.2R$) have peak values of $(\overline{B}_{\phi}^{\text{min}}, \overline{B}_{\phi}^{\text{max}}) = (-197, 216.7)\ \mathrm{kG}$.
- The values of B_{rms} are inside the range of the observations: $200\ \mathrm{G} - 30\ \mathrm{kG}$ (Braithwaite & Spruit, 2017).
- It seems that the core dynamo is not enough to create a large scale magnetic field.

Will a fossil field be enough to explain the observations in the surface of the star?

Future work

In order to create a more realistic model, we will include the hydrostatic equilibrium temperature profile from Käpylä et al. (2010):

$$T(r) = T_0 + \int_{r_0}^{r} \frac{|\vec{g}|}{c_{\mathrm{V}}(\gamma - 1)(m+1)} dr,$$

where:

$$m = \begin{cases} 1.5 & \text{if} \quad r < 0.2R \\ 3 & \text{if} \quad r > 0.2R \end{cases}$$

is the polytropic index.

Future work (1)

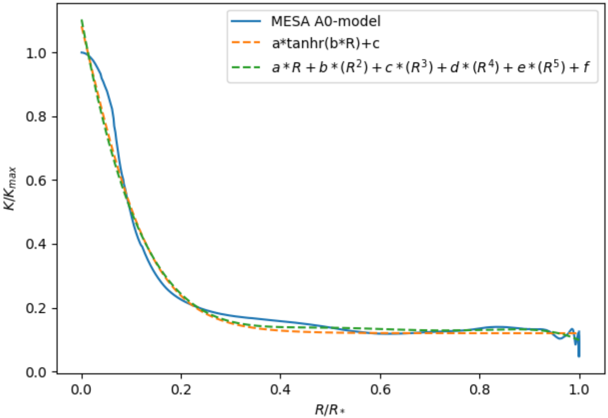

Figure: Heat conductivity radial profile created from the A0 main-sequence star MESA model.

Future work (2)

Profiles for diffusivities.

- We will incorporate non-constant values for the diffusivities.

Future work (2)

Profiles for diffusivities.

- We will incorporate non-constant values for the diffusivities. More specifically:

$$\nu_0 = 1.2 \cdot 10^8 \ \mathrm{m}^2/\mathrm{s}, \qquad \nu_{\mathsf{jump}} = 0.01$$
$$\eta_0 = 1.8 \cdot 10^8 \ \mathrm{m}^2/\mathrm{s}, \qquad \eta_{\mathsf{jump}} = 0.01$$

References

Augustson K. C., Brun A. S., Toomre J., 2016, , 829, 92

Babcock H. W., 1960, , 132, 521

Braithwaite J., Nordlund A., 2005, Astronomy and Astrophysics, 450

Braithwaite J., Spruit H. C., 2017, Royal Society Open Science, 4, 160271

Brandenburg A., Subramanian K., 2004, Phys. Rep., 417

Featherstone N. A., Browning M. K., Brun A. S., Toomre J., 2009, , 705, 1000

Käpylä P. J., Korpi M. J., Brandenburg A., Mitra D., Tavakol R., 2010, Astronomische Nachrichten, 331, 73

Käpylä P., 2021, Astronomy & Astrophysics, 651

Käpylä P. J., Gent F. A., Olspert N., Käpylä M. J., Brandenburg A., 2020, Geophysical & Astrophysical Fluid Dynamics, 114, 8

Navarrete F. H., Schleicher D. R. G., Käpylä P. J., Schober J., Völschow M., Mennickent R. E., 2019, Monthly Notices of the Royal Astronomical Society, 491, 1043

Padmanabhan T., 2001, Theoretical Astrophysics - Volume 2, Stars and Stellar Systems, by T. Padmanabhan, pp. 594. Cambridge University Press, July 2001. ISBN-10: 0521562414. ISBN-13: 9780521562416. LCCN: QB801 .P23 2001, vol. II

Paxton B., Bildsten L., Dotter A., Herwig F., Lesaffre P., Timmes F., 2010, The Astrophysical Journal Supplement Series, 192, 3

Pencil Code Collaboration et al., 2021, The Journal of Open Source Software, 6, 2807

Appendix A

Contributions to momentum and energy in the MHD equations:

- Viscosity

$$\vec{F}_{\text{viscous}} = \frac{1}{\rho}\vec{\nabla} \cdot [2\mu \boldsymbol{S}]$$

with:

$$S_{ij} = \frac{1}{2}(\partial_j u_i + \partial_i u_j) - \frac{1}{3}\delta_{ij}\vec{\nabla} \cdot \vec{u}$$

- Damping of flows

$$\vec{f}_d = -\frac{\vec{u}}{\tau_{\text{damp}}} f_e(r)$$

with:

$$f_e(r) = \frac{1}{2}\left(1 + \tanh \frac{r - r_{\text{damp}}}{w_{\text{damp}}}\right)$$

Appendix A (2)

- SGS entropy flux:

$$\vec{F}_{SGS} = -\chi_{SGS}\rho\vec{\nabla}s'$$

with:

$$s' = s - \langle s \rangle_t$$

- Explicit cooling and heating:

$$\mathcal{C}(\vec{x}) = \rho c_\mathrm{P} \frac{T(\vec{x}) - T_\mathrm{surf}}{\tau_\mathrm{cool}} f_e(r)$$

$$\mathcal{H}(r) = \frac{L_\mathrm{sim}}{(2\pi w_\mathrm{L}^2)^{3/2}} \exp\left(-\frac{r^2}{2w_\mathrm{L}^2}\right)$$

Appendix A (3)

- Gravitational potential:

$$\Phi(r) = -\frac{GM}{R}\frac{a_0 + a_2 r'^2 + a_3 r'^3}{1 + b_2 r'^2 + b_3 r'^3 + a_3 r'^4}$$

where $r' = r/R$, and $a_0 = 4.3641$, $a_2 = -1.5612$, $a_3 = 0.4841$, $b_2 = 4.0678$, $b_3 = 1.2548$ (Pencil code's *A0 star gravity potential*).

"Surface dynamos"

Sim3 $\Delta r \sim 0.3R, \Omega \approx 0.80\Omega_\odot$ (left) and $\Omega \approx 1.58\Omega_\odot$ (right):

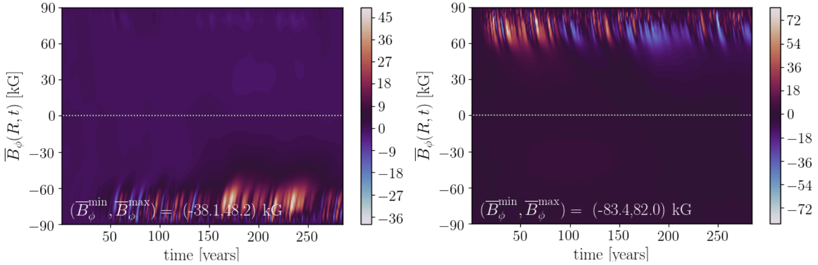

Figure: Azimuthal averaged magnetic field [kG] vs time [yr], at stellar surface, with $\nu = 2 \cdot 10^8\ \mathrm{m}^2/\mathrm{s}$, $\eta = 1.8 \cdot 10^8\ \mathrm{m}^2/\mathrm{s}$.

"Surface dynamos" (2)

Sim4 $\Delta r \sim 0.2R$, $\Omega \approx 1.24\Omega_\odot$ (left), and $\Omega \approx 2.48\Omega_\odot$ (right):

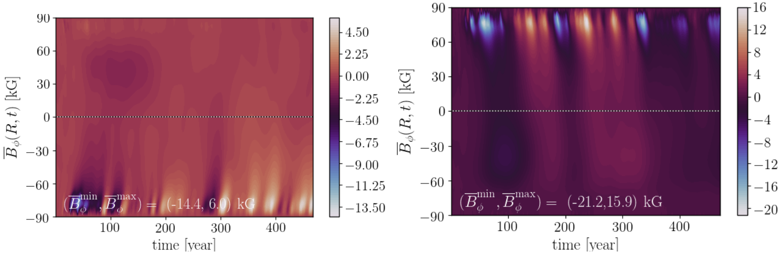

Figure: Azimuthal averaged magnetic field vs time, at stellar surface.

"Surface dynamos" (3)

Sim4 $\Delta r \sim 0.2R, \Omega \approx 6.20\Omega_{\odot}$:

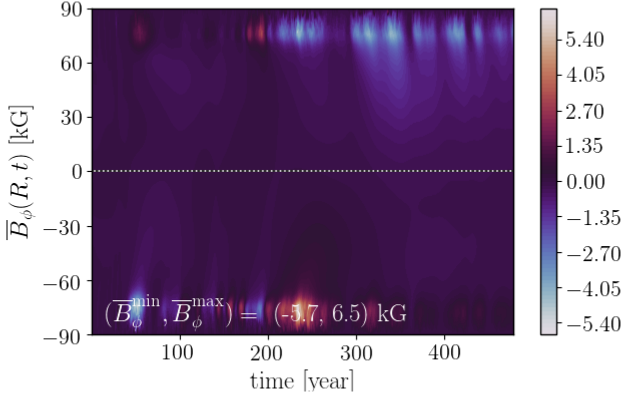

Figure: Azimuthal averaged magnetic field vs time, at stellar surface

Schwarzschild criterion

According to the Schwarzschild criterion, we can expect convection to occur if:

$$\vec{\nabla}_{\rm rad} = \frac{3}{16\pi acG}\frac{P}{T^4}\frac{\kappa l}{m} > \vec{\nabla}_{\rm ad}$$

This is:

- A large value of the opacity κ. Since low-mass stars are cooler than high-mass stars, we may expect low-mass stars to have convective envelopes.
- Regions with a large energy flux (i.e. large l/m), stars which nuclear energy production is strongly peaked towards the centre can be expected to have convective cores.

rms velocity of Sim4

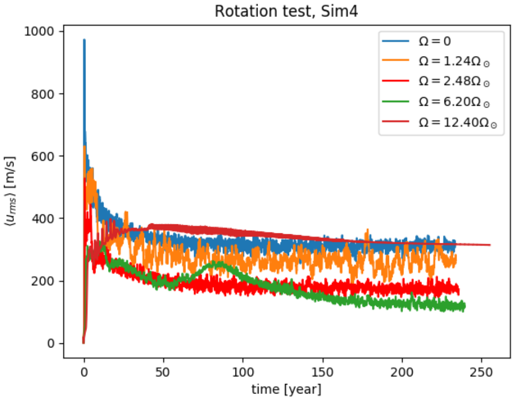

Figure: Volume averaged root-mean-square flow velocity [m/s] vs time [years] of runs from Sim4.